Low-Frequency Unsteadiness of Shock Wave/Turbulent Boundary Layer Interactions

Noel T. Clemens[1] and Venkateswaran Narayanaswamy[2]

[1]Department of Aerospace Engineering and Engineering Mechanics, The University of Texas at Austin, Austin, Texas 78712; email: clemens@mail.utexas.edu

[2]Department of Mechanical and Aerospace Engineering, North Carolina State University, Raleigh, North Carolina 27695

Annu. Rev. Fluid Mech. 2014. 46:469–92

The *Annual Review of Fluid Mechanics* is online at fluid.annualreviews.org

This article's doi:
10.1146/annurev-fluid-010313-141346

Keywords

supersonic, separation, bubble, reattachment, instability

Abstract

Shock wave/boundary layer interactions occur in a wide range of supersonic internal and external flows, and often these interactions are associated with turbulent boundary layer separation. The resulting separated flow is associated with large-scale, low-frequency unsteadiness whose cause has been the subject of much attention and debate. In particular, some researchers have concluded that the source of low-frequency motions is in the upstream boundary layer, whereas others have argued for a downstream instability as the driving mechanism. Owing to substantial recent activity, we are close to developing a comprehensive understanding, albeit only in simplified flow configurations. A plausible model is that the interaction responds as a dynamical system that is forced by external disturbances. The low-frequency dynamics seem to be adequately described by a recently proposed shear layer entrainment-recharge mechanism. Upstream boundary layer fluctuations seem to be an important source of disturbances, but the evidence suggests that their impact is reduced with increasing size of the separated flow.

1. INTRODUCTION

Shock wave/turbulent boundary layer interactions (SBLIs) represent complex flow phenomena that are associated with a wide range of flows, including transonic airfoils, supersonic inlets, control surfaces of high-speed aircraft, missile base flows, reaction control jets, and overexpanded nozzles. Often the shock induces significant boundary layer separation, which leads to a highly unsteady flow field that can cause aircraft buffeting, inlet instability, severe thermal loading of hypersonic vehicles, and aerostructure fatigue when the pressure oscillations couple to panel resonant frequencies. SBLI is a topic that has seen extensive study over the past 50 years (Dolling 2001), and there already exist many excellent reviews of past work on this topic. Dolling (1993) and Smits & Dussauge (1996) reviewed work in supersonic SBLIs through the early to mid-1990s, including discussions of the unsteady flow fields and some early thoughts on driving mechanisms. Lee (2001) reviewed work on SBLIs on transonic airfoils, which differs in many ways from higher–Mach number interactions owing to the ability of acoustic waves to travel upstream and influence the interaction. Other notable reviews include those by Delery & Marvin (1986), Zheltovodov (1996), and Andreopoulos et al. (2000) and the recent edited books by Babinsky & Harvey (2011) and Doerffer et al. (2010). Dolling (2001) gave a perspective on what issues need to be addressed, including understanding the source of low-frequency unsteadiness, developing improved computational capabilities, investigating more complex three-dimensional (3D) flows, and developing techniques for active control of shock-induced turbulent separation. Knight & Degrez (1998), Knight et al. (2003), and Edwards (2008) reviewed computational work in this area, and not surprisingly, the advances over one decade are quite remarkable.

SBLI unsteadiness is characterized by a wide range of frequencies, which encompass those characteristic of the upstream boundary layer as well as motions that are typically one to two orders of magnitude lower. Low-frequency, large-scale motions have attracted the most interest over the past two decades because they are the most challenging to model with numerical simulations, particularly with Reynolds-averaged Navier-Stokes methods (Dolling 1998). The obvious limitations of these computations have led to several recent studies that have employed direct numerical simulation (DNS) and large-eddy simulation methods, with great success, as highlighted below (Pirozzoli & Grasso 2006; Wu & Martin 2008; Touber & Sandham 2009, 2011; Morgan et al. 2010; Priebe & Martin 2012).

The low-frequency, large-scale motions have also been of interest because to date they have defied a definitive explanation as to why they occur. Even though there are sound technological reasons for seeking an understanding of the source of the low-frequency unsteadiness, there is no question that a major motivating factor for researchers is that we simply should be able to understand the supersonic flow over a 2D compression ramp, for example. Clearly, lacking this understanding puts into doubt our ability to explain significantly more complex flows, such as inlet-isolator shock trains.

In this review, we are specifically concerned with investigations over the past few decades that have sought to understand the source of the low-frequency unsteadiness of shock-induced turbulent separation in canonical flow fields. We first discuss some of the general unsteady characteristics of shock-induced turbulent separated flows and then discuss studies that provide evidence for either an upstream forcing mechanism or a downstream one. We conclude by proposing a viewpoint that seems to reconcile these apparently opposite views.

2. GENERAL FEATURES OF UNSTEADY MOTIONS

SBLIs have been studied in many different canonical geometries, such as those induced by compression ramps (swept and unswept), reflected shocks, glancing shocks, cylinders, and blunt and

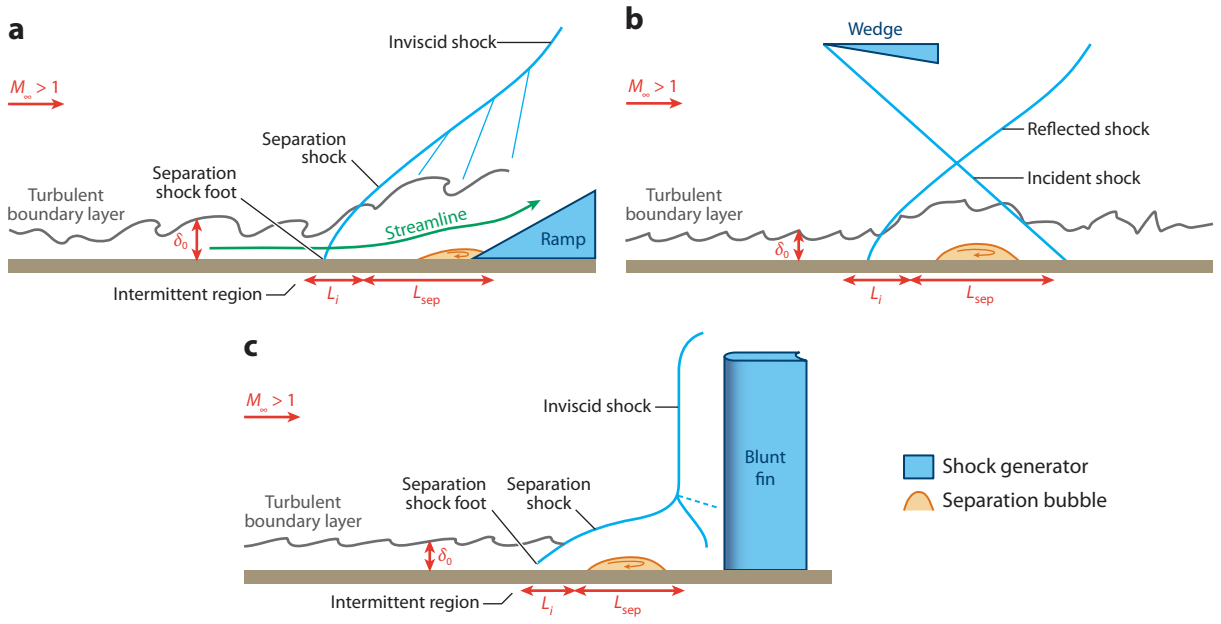

Figure 1

Schematic diagrams of three canonical shock wave/boundary layer interactions: (*a*) compression ramp, (*b*) reflected shock, and (*c*) blunt fin.

sharp fins. The remarkable feature of these flows is that they exhibit strong similarities in their unsteady motions (Smits & Dussauge 1996). **Figure 1** shows three canonical interactions: the compression ramp, reflected shock, and blunt-fin interactions. The first two interactions are nominally 2D, whereas the blunt-fin interaction is 3D, but all three are closed in the sense that fluid in the separation region recirculates upstream. In contrast, swept-ramp and sharp-fin interactions are 3D, but also open, because separated fluid is not trapped in a separation bubble but is continuously swept downstream in a large-scale vortical motion (Knight et al. 1987, Knight & Degrez 1998). The focus of this review is primarily on closed interactions as shown in **Figure 1**, but we demonstrate shortly below that there are gross similarities between open and closed separated flows, which suggest that the physics are at least broadly similar.

The mean structure of nominally 2D closed interactions can be understood by considering compression ramps of varying ramp angle. When the ramp angle is small, the adverse pressure gradient is not strong enough to separate the upstream boundary layer of thickness δ_0, free-stream velocity u_∞, and free-stream Mach number M_∞. As the ramp angle increases, at some point a small separation bubble begins to form, and the oblique shock begins to stand off from the corner, which is the condition of incipient separation (Settles et al. 1979). As the ramp angle is increased further, the bubble grows, the shock moves progressively further upstream, and the separation length scale L_{sep} increases. The magnitude of separation depends on the ramp angle (the strength of the inviscid disturbance) and the Reynolds number of the upstream boundary layer (because it is a measure of the ability of the boundary layer to resist separation). The upstream boundary layer separates from the wall upstream of the separation bubble and lifts over the bubble. The upward deflection of the flow upstream of the separation bubble leads to the formation of the separation shock wave. The lowest part of the separation shock (where it terminates at the sonic line) is called the separation shock foot. The separation shock foot oscillates back and forth over a

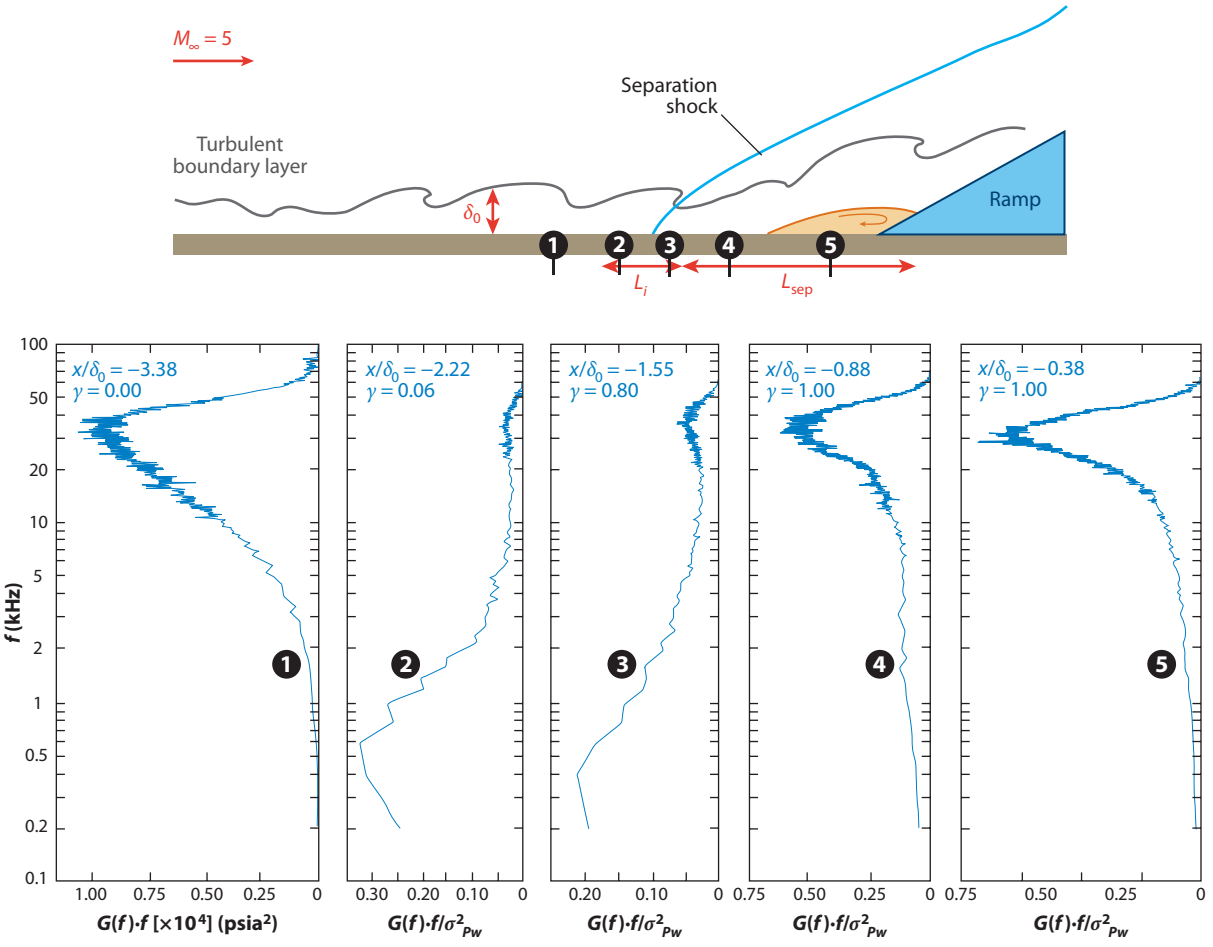

Figure 2

Pressure power spectra underneath the interaction generated by a 28° compression ramp in a Mach 5 flow. Figure adapted from Erengil & Dolling (1991b) with permission of the American Institute of Aeronautics and Astronautics.

region of length L_i called the intermittent region. In the case of the compression ramp and blunt fin, the separation shock tends to be considerably weaker than the inviscid shock.

The unsteady characteristics of the separation shock and separation bubble motions exhibit strong similarities across all separated interactive flows. For example, in compression ramp interactions, many researchers have made fluctuating pressure measurements at discrete locations underneath the interaction (Dolling & Murphy 1983, Andreopoulis & Muck 1987, Erengil & Dolling 1991b, Thomas et al. 1994, Ringuette et al. 2009). **Figure 2** shows example power spectra taken by Erengil & Dolling (1991b) in a Mach 5 compression ramp interaction at five different stations. Station 1 is under the upstream boundary layer, and the pressure fluctuations are high frequency and peak near the outer-scale frequency, U_∞/δ_0. Stations 2 and 3 are underneath the intermittent region and exhibit a dominant peak at a very low frequency of approximately 500 Hz, which is of order $0.01U_\infty/\delta_0$. This is known to represent the dominant oscillation frequency of the separation shock foot. Station 4 is underneath the separation bubble, and the frequencies are high, once again, as they are affected by radiation from the turbulent shear layer above. These same basic

trends in the fluctuating pressure field hold for other interactions, including those generated by blunt and sharp fins, ramps with sweep, and reflected shocks (Schmisseur & Dolling 1994; Erengil & Dolling 1993a; Brusniak & Dolling 1994; Smits & Dussauge 1996; Dupont et al. 2005, 2006).

Measurements show that the intermittent-region frequencies decrease as the magnitude of separation (L_{sep}) increases. Generally, L_i increases with L_{sep}, so the shock foot undergoes larger-scale motion as the scale of separation increases. Gonsalez & Dolling (1993) made measurements (and compiled data from previous studies) in a wide range of SBLIs, including blunt fins, sharp fins, and compression ramps, all with varying sweep angles. Fluctuating wall-pressure data were used to determine mean and root-mean-square pressure, pressure power spectra, intermittent region lengths, and shock-foot velocity. Owing to the varying sweep angles, a wide range of separated flow length scales was studied. Furthermore, both closed (unswept-ramp and blunt-fin) and open (swept-fin and swept-ramp) separated flows are represented by the configurations considered. **Figure 3*a*** shows the maximum zero-crossing frequency versus intermittent region length. The zero-crossing frequency, f_c, is the number of times that the shock foot passes back and forth across a transducer in 1 s. This frequency varies across the intermittent region, and what is shown in the figure is the peak value, $(f_c)_{max}$. This figure shows that shock oscillation frequencies decrease with increasing intermittent region length. However, when the peak frequency is nondimensionalized in the form of the Strouhal number with the intermittent region length as the characteristic length scale, $St_{Li} = (f_c)_{max} L_i/U_\infty$, then the trend in **Figure 3*b*** is obtained. **Figure 3*b*** shows St_{Li} as a function of sweep angle (λ_s). It is quite striking that all the interactions from fins and ramps with varying amounts of sweep exhibit a similar Strouhal number, whose value lies within the range $St_{Li} \approx 0.01$ to 0.03.

Gonsalez & Dolling (1993) also used the pressure data to compute the shock-foot position history, from which they derived the shock velocity, U_s (see Erengil & Dolling 1993b for sample time histories of the shock velocity). The mean shock velocity U_s is shown in **Figure 3*c***, as a function of L_i, for a number of different interactions. This figure is also quite striking as it shows that the mean shock-foot velocity varies by only a factor of 2 for a factor of 6 variation in L_i, and the mean velocity is essentially the same for upstream and downstream sweeps of the shock foot. The value of the shock velocity ranges from 2% to 4% of U_∞ regardless of the interaction geometry or separated flow scale. The shock moves at a slow speed in the laboratory frame of reference, but it is of course supersonic with respect to the free-stream flow. **Figure 3*d*** is adapted from the data presented in Gonsalez & Dolling (1993) and shows frequency-multiplied pressure power spectra (normalized by the root-mean-square pressure) underneath the intermittent region as a function of the Strouhal number for different interactive flows. We see that there is general collapse of the spectra among the interaction types, in that they exhibit peak energy at Strouhal numbers in the range of 0.01 to 0.03. The general similarity of the interactions suggests that the physics of separation shock motion unsteadiness is similar over a wide range of interactive flows. It is seen, however, that the unswept compression ramp and blunt-fin interactions seem to have lower peak Strouhal numbers than the swept interactions. This difference is potentially interesting because it may reflect a difference in the unsteady motions for closed separated flows (unswept ramps and blunt fins) and open ones (swept ramps and fins). Because closed interactions have trapped recirculating fluid, they potentially have a feedback path that is more dominant than in open interactions. Although this possible difference between closed and open interactions could be important, the unsteadiness of open interactions is not well understood, so this review focuses primarily on the closed type.

Although the various features of the shock motion discussed above are interesting, we note that the separation shock motions are driven by the separated flow unsteadiness, as shown by Erengil & Dolling (1991b). Hence, the question that we want to explore in this review is, what drives the large-scale pulsations of the separated flow? Historically, most relevant studies have come down on one of two sides: The driving mechanism of low-frequency unsteadiness is forcing by

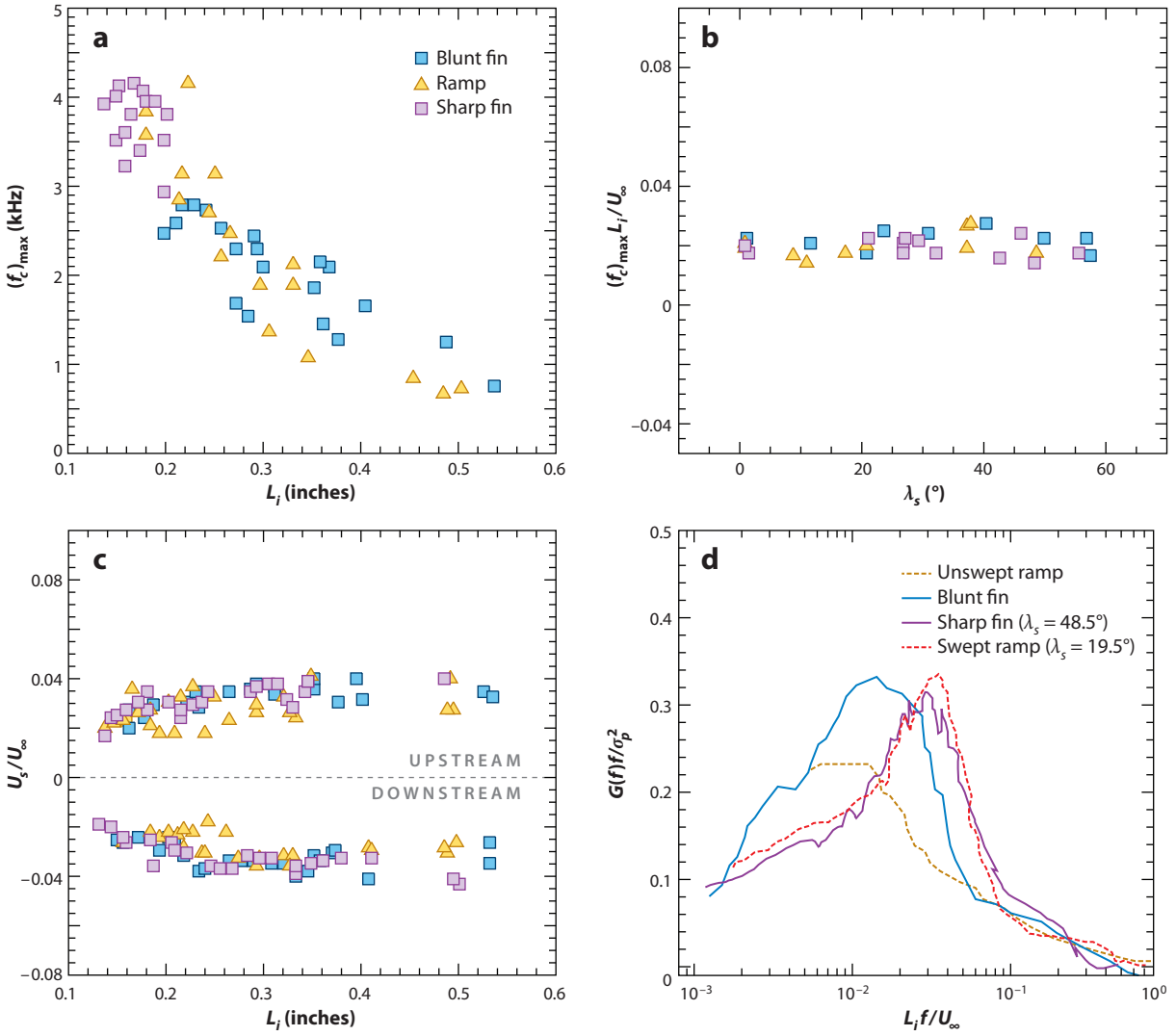

Figure 3

Data from fluctuating wall-pressure measurements for different shock wave/boundary layer interactions: (*a*) maximum shock zero-crossing frequency $(f_c)_{max}$ versus L_i, (*b*) Strouhal number $St_{Li} = (f_c)_{max} L_i/U_\infty$ versus sweep angle λ_s, (*c*) normalized shock velocity U_s/U_∞ versus L_i, and (*d*) power spectral density versus Strouhal number. Figure adapted with permission from Gonsalez & Dolling (1993).

the upstream turbulent boundary layer, or it results from an intrinsic instability of the separated flow. We now survey the evidence for each mechanism in the following two sections and discuss the growing consensus that is emerging regarding this important problem.

3. UPSTREAM MECHANISM

An obvious place to look for the source of unsteadiness of shock-induced separation is the upstream turbulent boundary layer; however, traditionally, it had been difficult to reconcile the low

frequencies observed in the intermittent region (of order 0.01 to $0.1U_\infty/\delta_0$) with a conventional turbulent mechanism. Plotkin (1975) proposed a mathematical model that assumed that the shock is displaced (convected) by velocity fluctuations in the upstream boundary layer and that it tended to become restored to its mean location owing to the stability of the mean flow field. Under the assumption that the timescale of velocity fluctuations is much smaller than the timescale of the shock motion (which is generally true owing to the slow shock speeds of order 3% of U_∞), his model shows that low-frequency motion can result from high-frequency forcing in analogy to a random-walk process. Recently, Poggie & Smits (2001) showed that experimental wall-pressure data were consistent with Plotkin's model, except in regions characterized by low-frequency pressure fluctuations. In such regions, the requirement that the turbulent eddy timescales be much smaller than the shock motion is less likely to be true, if we accept an upstream mechanism. In a related study, Touber & Sandham (2011) developed a first-order model similar to Plotkin's and showed that when this simplified system was forced with white noise, the resulting large-scale motions of the interaction were remarkably similar to those observed experimentally and numerically. Although Touber & Sandham (2011) argued that the separated flow dynamics do not require an upstream source of forcing, the upstream boundary layer is a natural source of broadband fluctuations of the type that is needed to drive the low-frequency unsteadiness of the system. In fact, when the authors high-pass filtered the forcing function to remove low-frequency content, the system did not exhibit low-frequency oscillations.

Among the first to experimentally investigate an upstream boundary layer mechanism were Andreopoulos & Muck (1987), who made wall-pressure measurements under a Mach 3 compression ramp interaction. They measured the time between shock crossings across a transducer within the intermittent region and determined the mean shock-crossing time period, T_m. The shock zero-crossing frequency, $f_c = 1/T_m$, was found to exhibit a Strouhal number $\mathrm{St}_\delta = f_c\delta_0/U_\infty = 0.13$, which they claimed to be of the same order of magnitude as the upstream boundary layer bursting frequency. Furthermore, from T_m, they inferred the mean shock speed and argued that it is of the same order as the upstream velocity fluctuations, which provided further evidence for an upstream forcing mechanism. Later, Dolling & Brusniak (1989) showed that the single threshold technique used by Andreopoulos & Muck (1987) to detect shock passage was susceptible to misinterpreting turbulent fluctuations as shock passage motions. Owing to this, their data likely exhibited zero-crossing frequencies that were too high.

Erengil & Dolling (1993b) studied a Mach 5 28° compression ramp interaction and used pressure measurements under the intermittent region to obtain time histories of the shock-foot position and velocity. They observed a clear correlation between the shock-foot velocity and the pressure fluctuations in the upstream boundary layer. The nature of the correlation indicated that the passage of upstream pressure fluctuations preceded the shock-foot motion. Furthermore, the same correlation was observed in swept compression ramp interactions; however, correlations between the pressure under the separated flow region and the intermittent region indicated that motions in the separation bubble preceded the shock-foot motion. This led them to argue that the shock-foot motion is driven by two mechanisms: the upstream boundary layer, which causes a high-frequency smaller-scale jitter motion, and large-scale pulsations of the separation bubble, which induce large-scale motions of the separation shock foot. However, they were not able to determine what drives the large-scale pulsations of the separation bubble. This result led them to conclude that the separation shock responds to pulsations of the separation bubble, as was suggested by Erengil & Dolling (1993b).

Brusniak & Dolling (1994) performed simultaneous high-frequency wall-pressure measurements in a Mach 5 blunt-fin interaction. Correlations of fluctuating wall pressure were measured between locations in the upstream boundary layer and various downstream locations. The

cross-correlation curve between fluctuations in the upstream boundary layer and under the intermittent region had two characteristic peaks: a sharp peak at a positive time delay that corresponds to the passage of convected turbulent structures and a broad negative peak at a positive time delay that corresponds to the shock-foot unsteadiness. Because both correlation peaks were at a positive time delay, the upstream boundary layer fluctuations preceded the downstream motions. That the intermittent region correlation peak is negative means that positive fluctuations in the upstream boundary layer are correlated with negative fluctuations in the intermittent region, and vice versa. Negative pressure fluctuations are associated with downstream shock motion because the pressure decreases as the shock moves downstream of the transducer.

For correlations between the upstream boundary layer transducer and one under the separated flow, the authors obtained a sharp peak (owing to the convection of turbulent structures) as well as a broad positive peak. The broad positive peak is at a positive time delay, which also means that fluctuations under the separated flow are preceded by fluctuations in the upstream boundary layer. We also note that the positive value of the correlation peak implies that positive boundary layer pressure fluctuations cause positive fluctuations under the separation bubble. We would expect the downstream transducer pressure to rise as the separated flow contracts, as this would bring the reattachment point closer to the transducer. These measurements are consistent with those of Thomas et al. (1994), who argued that the separation bubble expands and contracts in a manner such that the downstream motion of the separation shock is correlated with the upstream motion of the reattachment point, and vice versa. As a means to determine whether the correlations stemmed from high- or low-frequency events in the upstream boundary layer, Brusniak & Dolling (1994) high-pass filtered the wall-pressure signals from the upstream boundary layer before computing the cross-correlations. When this high-pass signal was correlated with the wall-pressure signal at subsequent downstream locations, the broad peak that was originally present disappeared. The authors concluded, "The most obvious result is that a correlation *does* exist between signals from under the incoming undisturbed boundary-layer flow and both the intermittent and separated flow regions."

McClure (1992) studied the effect of upstream turbulent fluctuations on a Mach 5 28° compression ramp interaction by using wall-pressure measurements. He ensemble averaged the pressure data based on upward or downward sweeps of the separation shock foot within the intermittent region. His ensemble-average results showed that shock sweeps were clearly associated with particular pressure signatures in the upstream boundary layer. Gramman & Dolling (1992) studied the structures responsible for these sweeps and showed that they could be detected up to $20\delta_0$ upstream of the interaction. Both McClure (1992) and Gramman & Dolling (1992) showed that upstream and downstream shock-foot sweeps were associated with falling and rising Pitot pressure in the upstream boundary layer, respectively. Based on these and other results, Ünalmis & Dolling (1994) proposed that a low-frequency thickening/thinning motion in the upstream boundary layer causes upstream/downstream sweeps of the separation shock foot.

Beresh et al. (2002) sought to test Ünalmis & Dolling's (1994) thickening/thinning mechanism by acquiring velocity data using the particle image velocimetry (PIV) technique in the upstream boundary layer together with simultaneous wall-pressure data under the intermittent region to infer the separation shock-foot motion. They also ensemble averaged the upstream velocity fluctuations conditioned upon upstream or downstream sweeps of the separation shock foot and found a clear and systematic trend. **Figure 4** shows ensemble-average velocity fluctuation (u') profiles conditioned on different shock motions: no motion; upstream sweeps across one, two, and three transducers; and downstream sweeps across one, two, and three transducers. Note that if there is no correlation between the upstream velocity fluctuations and the shock motion, then the profiles will average to zero (i.e., $\overline{u'} = 0$). The profiles in the figure show that the mean fluctuations for all cases are approximately zero in the outer part of the boundary layer, which means that the

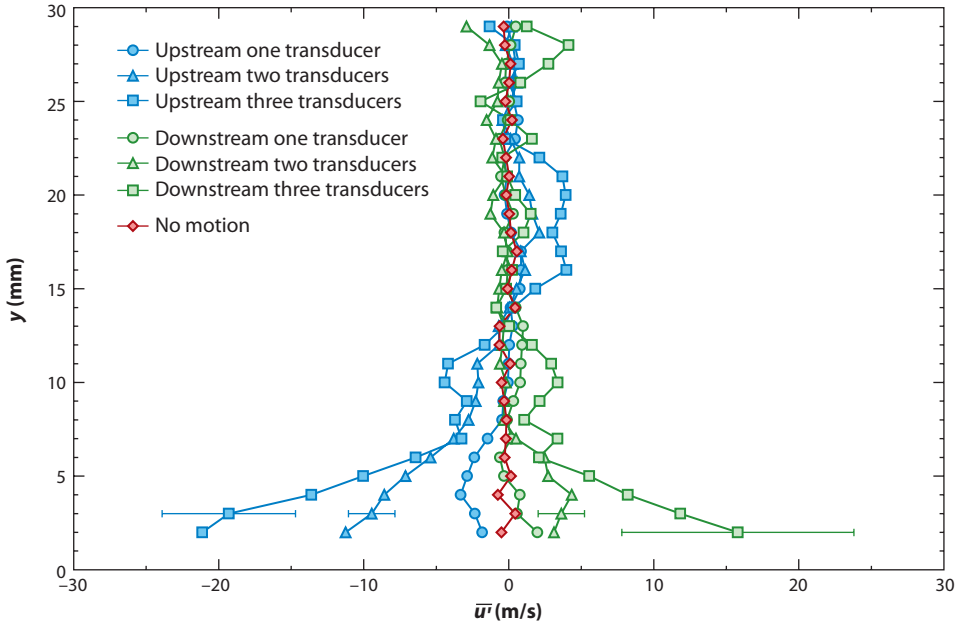

Figure 4

Conditional ensemble-average profiles of the streamwise velocity fluctuations in the incoming boundary layer conditioned on the separation shock-foot motion within a time period of 250 μs. Figure taken from Beresh et al. (2002), adapted with permission of the American Institute of Aeronautics and Astronautics.

velocity fluctuations at that location are uncorrelated with particular types of shock-foot motion. However, closer to the wall, the mean fluctuations deviate substantially from zero, particularly for larger shock sweeps. The observed trend implies that downstream and upstream shock sweeps are associated with positive and negative velocity fluctuations, respectively, in the lower part of the upstream boundary layer. The trend clearly gets stronger closer to the wall, but because the PIV measurements were not reliable below approximately 2 mm from the wall, it is not known how much larger the conditional fluctuations would get. Beresh et al. used this figure to conclude that the shock foot responds to changes in the instantaneous momentum in the upstream boundary layer: In other words, an instantaneously fuller profile leads to downstream shock motion, and an instantaneously retarded profile leads to upstream shock motion. Hou et al. (2003) made PIV measurements in a Mach 2 compression ramp interaction simultaneously with wall-pressure measurements and showed large differences in the interaction scale when the shock foot was upstream versus downstream. Hou (2003) conducted a similar analysis to Beresh et al. (2002) and showed that the upstream velocity profiles were fuller, by approximately $0.04u_\infty$, when the shock foot was downstream as compared to when it was upstream.

Ganapathisubramani et al. (2007) conducted plan-view (streamwise-spanwise plane) PIV imaging in the boundary layer upstream of a Mach 2 compression ramp interaction. They observed the presence of long regions of low-velocity fluid in the log region that remained coherent for at least 8δ (the size of the imaging field of view). These superstructures were shown to be quite similar in character to those observed in the log region of incompressible boundary layers (Hutchins & Marusic 2007). Subsequently, Ganapathisubramani et al. (2009) conducted 6-kHz PIV measurements of the same flow and used the time-resolved movie sequences to create a pseudoinstantaneous snapshot of the upstream velocity field by the application of Taylor's

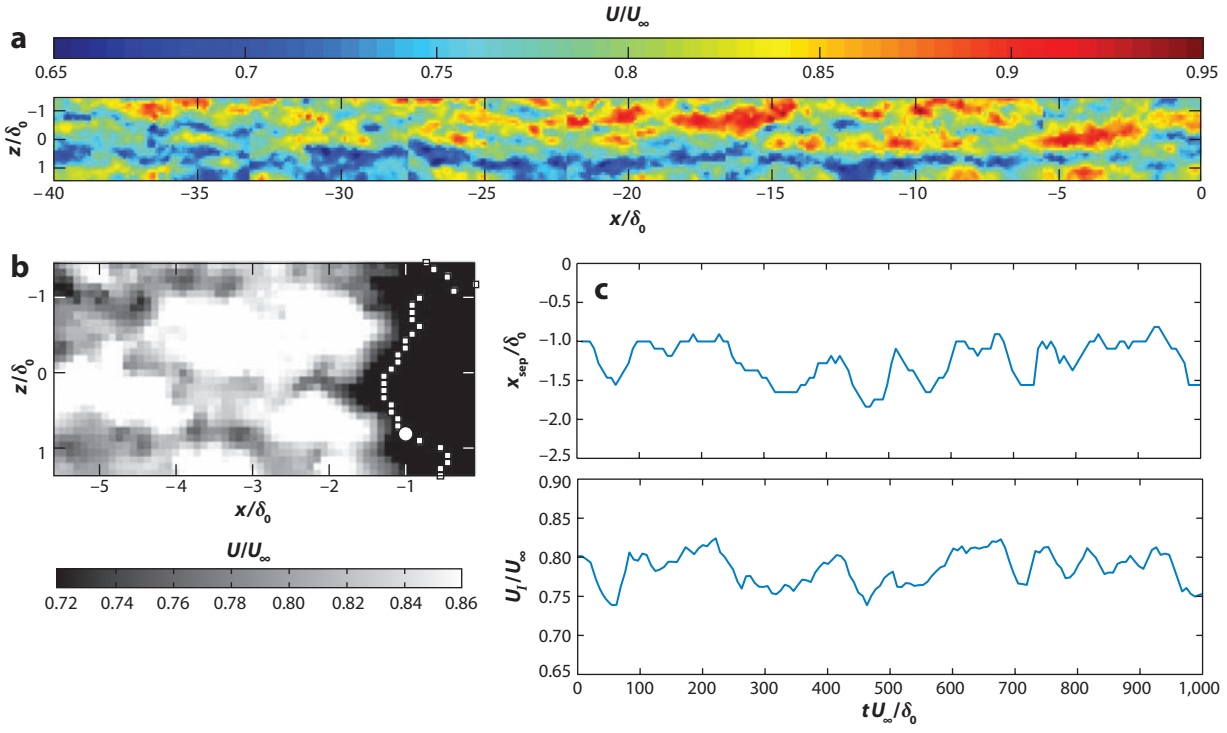

Figure 5

Sample time-resolved streamwise-velocity data (*u* velocity) acquired using PIV in a Mach 2 compression ramp interaction. (*a*) Time sequence of plan-view (streamwise-spanwise) velocity contour plots that have been shifted by the convection distance to form a pseudoinstantaneous snapshot of the upstream boundary layer structure. (*b*) Streamwise velocity field near the separation region. The dotted line is the separation line surrogate. The large white dot is the location upstream of which the velocity data were averaged to obtain the correlation between U_l and $x_{sep.}$ (*c*) Sample time histories obtained in a Mach 2 compression ramp interaction. (*Top panel*) Low-pass filtered separation surrogate (x_{sep}). (*Bottom panel*) Upstream velocity averaged along a streamwise line upstream of the separation location (U_l). The velocity is normalized by the free-stream velocity (U_∞). Figure adapted with permission from Ganapathisubramani et al. (2009). Copyright © 2009 Cambridge University Press.

hypothesis. **Figure 5*a*** shows a sample contour plot of the *u* velocity, demonstrating that the superstructures can exhibit coherence to lengths as large as $40\delta_0$. Ganapathisubramani et al. (2007, 2009) investigated the effect of these structures on the separated flow dynamics by defining a separation line surrogate (based on a particular low-velocity contour) and relating it to the fluctuations in the upstream boundary layer (**Figure 5*b***). They observed a very strong correlation between the line-averaged upstream velocity (U_l) and the instantaneous position of the separation line surrogate (x_{sep}). **Figure 5*c*** compares time series of $x_{sep}(t)$ and $U_l(t)$. The two time histories are seen to be strongly correlated, and the computed peak correlation coefficient is approximately 0.75. This line average filters out smaller-scale fluctuations and so effectively highlights the influence of the large-scale coherent structures (without low-pass filtering, the peak correlation coefficient is 0.6). Their time-resolved PIV measurements also enabled them to observe that the upstream boundary layer exhibited a very-low-frequency motion that affected the entire span of the field of view and so did not result from superstructures. To investigate this effect, they averaged the upstream velocity over the entire span and compared this average to the mean separation line surrogate location. In this case, they also found a strong correlation, which indicates that global velocity fluctuations are

also important for driving the separation surrogate. Based on these findings, they concluded that the separation line oscillates in response to a combination of local upstream influences (namely, superstructures) and global influences, which could include very-low-frequency oscillations of the upstream boundary layer, as well as downstream separation bubble effects.

Researchers at Delft University have made extensive planar and tomographic PIV measurements in a Mach 2.1 impinging shock interaction (Humble et al. 2007a,b,c, 2009). Humble et al. (2009) specifically addressed the issue of the influence of the upstream boundary layer. Their 3D technique enabled them to observe that hairpin-type vortical structures are associated with low-momentum regions, consistent with the hairpin-packet model proposed by Kim & Adrian (1999), Adrian et al. (2000), and Tomkins & Adrian (2003). They further observed the presence of elongated low-speed structures in the upstream boundary layer, and the separated flow was shown to conform to the presence of the structures. However, they noted that the spanwise organization is not found in many realizations. They conducted a similar analysis to that of Ganapathisubramani et al. (2007) and investigated the relationship between upstream velocity fluctuations and a separation line surrogate (also based on a low-velocity contour). Their results also show a clear correlation between upstream velocity fluctuations and the surrogate separation location. The correlation coefficient was computed to be 0.5, which is consistent with those obtained by Ganapathisubramani et al. (2007) and Wu & Martin (2008), 0.4 and 0.5, respectively. Based on their observations, the Delft University researchers proposed that the wrinkling of the separated flow is caused by the spanwise organization of the structures in the incoming boundary layer, and the streamwise motion is caused by the changes in the bulk momentum of the incoming flow.

4. DOWNSTREAM MECHANISM

Although the evidence for the influence of the upstream boundary layer is quite compelling, there are also many studies that have failed to detect any upstream influence on the interaction unsteadiness or have shown that a downstream source is more prominent. For example, many studies have used wall-pressure measurements to correlate pressure fluctuations in the upstream boundary layer, under the intermittent region, under the separated flow, and near reattachment. Several of these studies have observed both upstream and downstream influences. For example, Erengil & Dolling (1991a, 1993b), Gramman & Dolling (1990), and Brusniak & Dolling (1994) observed distinct correlations between pressure fluctuations in the upstream boundary layer and shock-foot unsteadiness. They also reported correlations between shock-foot motion and pressure fluctuations under the separation bubble. However, the downstream pressure fluctuations were observed to precede the shock-foot motion. These observations have led subsequent researchers to conclude that this proves that the separated flow drives the interaction unsteadiness, but Brusniak & Dolling (1994) pointed out that such conclusions should be made with caution because it is possible that upstream structures could influence the separated flow, which in turn could displace the separation shock foot.

In response to the findings of Andreopoulis & Muck (1987), Thomas et al. (1994) investigated the role of burst-sweep events in the upstream boundary layer on the dynamics of a Mach 1.5 compression ramp interaction. The ramp angles were relatively small (6–12° angles), and the interaction was approximately $2\delta_0$ in length. They used a filtering approach to isolate burst-sweep events and to correlate those to the shock motion; however, they observed no correlation between the two phenomena. Their measurements further suggested that the separation bubble expands and contracts in such a way that the separation and reattachment points move in opposite directions. Furthermore, the observation that the reattachment region fluctuations are highly coherent with the fluctuations in the intermittent region indicated a downstream source for the unsteadiness.

Pirozzoli & Grasso (2006) used DNS to simulate a Mach 2.25 impinging shock interaction. Their simulation did not extend to long-enough times to capture the lowest-frequency motions observed in the experiments, so this issue could not be addressed. However, they observed that the interaction oscillates with specific tones, which they argued were similar to Rossiter modes in cavity flows. Owing to these observations, the authors proposed that an acoustic feedback mechanism plays a role in driving the separated flow unsteadiness, although this would mainly act at higher frequencies than those associated with the largest-scale motions.

Touber & Sandham (2009) performed large-eddy simulations of the impinging SBLI configuration with an 8° shock generator to simulate the experiments by Dupont et al. (2005). Their simulations made fair predictions of the boundary layer parameters, mean separation length scale, and power spectral density of the wall-pressure fluctuations in the different regions of the impinging SBLI. Particularly, they were able to reproduce the low-frequency unsteadiness of the SBLI in the intermittent region and power spectrum at the incoming boundary layer with very good accuracy. They analyzed the incoming boundary layer structures at $y/\delta_0 = 0.2$ and showed the absence of the superstructures found by Ganapathisubramani et al. (2007). In fact, the typical length scale of the turbulent structures at $y/\delta_0 = 0.2$ was an order of magnitude smaller than that needed to cause low-frequency pulsations. That the low-frequency pulsations still existed despite the absence of the superstructures led them to conclude that the superstructures play a minor role in driving the SBLI pulsations. Furthermore, using linear stability analysis, these authors identified a node of instability inside the separation bubble that can generate a low-frequency upstream propagating disturbance with a convective velocity of the order $0.05U_\infty$. The similarity between the frequency of the disturbance from the node and the low-frequency pulsations of the SBLI and the similarity between the convective velocity of the disturbance and the shock velocity suggested to the authors that the global instability inside the separation bubble may be a possible driving mechanism of the SBLI.

Over the past decade, the topic of the SBLI driving mechanism has been extensively studied experimentally at the Université de Provence/UMR CNRS in Marseille, with a focus on reflected shock interactions. For example, Dupont et al. (2005) measured the coherence between the wall-pressure fluctuations near the vicinity of the reflected shock and those near the reattachment region and found it to be greater than 0.8. This high coherence led the researchers to conclude that the separation bubble and the separation shock oscillate as a quasi-linear system. Although such high coherence between the reattachment point and separation shock motion does not preclude an upstream mechanism, as pointed out by Brusniak & Dolling (1994), it would certainly be expected if reattachment-point fluctuations drive the separated flow unsteadiness.

In later studies, Piponniau et al. (2009) and Souverein et al. (2010) sought to determine if they could observe differences in the upstream boundary layer profiles for different separated flow length scales in different reflected shock interactions. In the case of Souverein et al. (2010), the interactions varied from "incipiently" separated flows (defined in their paper as having no mean reverse flow as measured by PIV) to more strongly separated interactions with substantial mean reverse flow. Note that their definition of incipient differs from that of Settles et al. (1979), and this topic is discussed further in Section 5. They studied two incipient cases, one with $M_\infty = 2.3$ and $\mathrm{Re}_\theta = 5{,}000$ and the other with $M_\infty = 1.7$ and $\mathrm{Re}_\theta = 50{,}000$. Different shock-generator wedge angles were used to generate similar strength interactions ($L/\delta_0 \approx 2.2$, where L is the interaction length). The more strongly separated cases were all at the lower Reynolds number and had measured relative interaction lengths of $L/\delta_0 \approx 4.2$ and 6.5. Souverein et al. (2010) measured the conditionally averaged upstream velocity profiles for cases of small and large separation bubbles and showed that the upstream boundary layer was indeed on average slightly fuller when the separation bubble was small. This effect was largest for the incipient cases (3% to

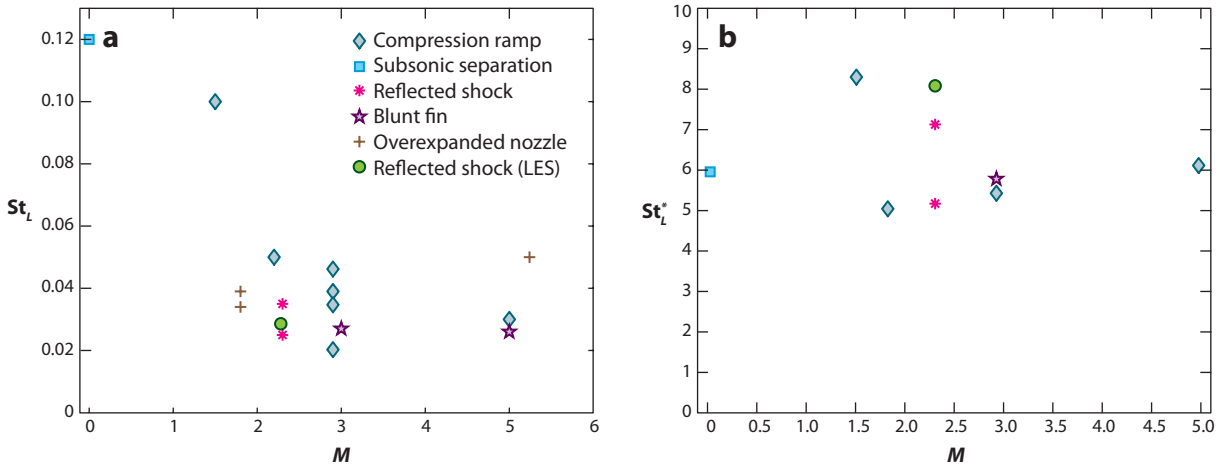

Figure 6

Strouhal number scaling of the low-frequency motion of several different turbulent separated flows. (*a*) Conventional Strouhal number scaling based on u_∞ and the interaction length, L. (*b*) Modified Strouhal number scaling accounting for entrainment differences. Figure adapted with permission from Piponniau et al. (2009). Copyright © 2009 Cambridge University Press.

4% of U_∞), and smaller for the stronger interactions (1% of U_∞). They concluded that fluctuations in the upstream boundary layer do influence the separated flow scale, but the effect weakens as the interaction becomes larger.

Further studies explored other potential mechanisms inside the separation bubble in impinging shock interactions. Dupont et al. (2006) conducted a detailed study of the space-time organization of the separated flow. They made simultaneous wall-pressure measurements with different separation distances between the transducers. Using these data, they were able to confirm the earlier findings of Dupont et al. (2005) about the coherency and phase relationship between the separation shock and separation bubble, and other locations inside the separation bubble. They also studied the power spectral density at different locations inside the separation bubble. From the evolution of the Strouhal number of the dominant frequency along the separation bubble, they found a similarity in the structure of a subsonic and supersonic separation bubble.

Piponniau et al. (2009) proposed a simple model of separation bubble unsteadiness that explicitly assumes the importance of the shear layer in terms of its entrainment characteristics. They assumed that the shear layer entrains the low-momentum fluid inside the separation bubble and hence depletes it of mass. Because the amount of mass in the bubble is constant if averaged over long times, they further argued that the bubble must have its mass recharged on a characteristic time $T =$ (mass in the reverse flow)/(rate of mass entrainment). They proposed that this recharge mechanism could be related to large-scale transverse motion (i.e., flapping) of the shear layer near the mean reattachment point. A similar mechanism based on entrainment considerations was also proposed by Wu & Martin (2008) for compression ramp interactions. Piponniau et al. (2009) assumed that the characteristic frequency of bubble oscillation is $f = 1/T$, and hence the Strouhal number formed with this frequency depends on the shear layer entrainment rate and the mass (and hence size) of the separation bubble. For example, **Figure 6*a*** shows the Strouhal number for the low-frequency motions of different separated flows as a function of free-stream Mach number. For the Strouhal number, they used the interaction length scale (L), which is a generic measure of interaction size that can be more readily determined from results in the legacy literature. **Figure 6*a***

shows that St_L exhibits a large amount of variation over the Mach number range of 0 to 5, and it is particularly clear that subsonic separated flows exhibit much higher oscillation frequencies than shock-induced separated flows. We note that the scaling used in **Figure 6*a*** is similar to the one used by Gonsalez & Dolling (1993), except Gonsalez & Dolling used the intermittent region length scale (L_i) as the characteristic length scale and their data were limited to Mach 5 free-stream conditions. These differences may explain the superior collapse of the data shown in **Figure 3*b***. Piponniau et al. (2009) hypothesized that the difference in oscillation frequencies across the Mach number range results from differences in the shear layer entrainment rate, and they developed a relation for a modified Strouhal number, $St_L^* = St_L f(r, s, M_c)$, which weights St_L by a function f that accounts for the effects of shear layer velocity ratio (r), density ratio (s), and compressibility (through the convective Mach number, M_c) on the entrainment rate. **Figure 6*b*** shows the same data in **Figure 6*a*** now plotted as a function of St_L^*, and we find that this scaling provides much improved collapse over the same Mach number range.

Wu & Martin (2008) and Priebe & Martin (2012) studied a Mach 2.9 24° compression ramp interaction by using DNS at $Re_\theta = 2{,}390$. Wu & Martin (2008) focused on correlating different quantities to the fluctuations of the separation shock. For example, they investigated the mechanism proposed by Ganapathisubramani et al. (2007, 2009) that there exists a strong correlation between fluctuations in the upstream boundary layer and the separated flow motion. They tested the separation line surrogate used by Ganapathisubramani et al. (2007, 2009) to see if it provided a correlation to upstream mass flux fluctuations. Indeed, a significant correlation was obtained as the peak correlation coefficient was 0.5, which was in excellent agreement with the measurements of Ganapathisubramani et al. (2007) and Humble et al. (2007b, 2009), who reported peak correlation coefficients of 0.4 and 0.5, respectively. However, Wu & Martin (2008) pointed out that the separation line surrogate does not necessarily represent the true separation line. To test this, they compared the correlation of the upstream mass flux fluctuations with the true separation point position history (determined as the location at which the skin friction was zero). They noted that the correlation at $y/\delta = 0.2$ is significantly weaker (correlation coefficient of 0.23) than that with the separation surrogate (coefficient of 0.5). This finding suggests that the separation surrogate may significantly overestimate the magnitude of the correlation. However, the correlation coefficient between mass flux fluctuations in the upstream boundary layer and the true separation point fluctuations peaked at a value of 0.3 near the wall, which shows that a significant correlation exists even though it is overestimated by the separation line surrogate.

Wu & Martin (2008) also correlated the time histories of the true separation point and separation shock (at the edge of the boundary layer) and found that the separation point and separation shock oscillate virtually in lockstep, as inferred by Erengil & Dolling (1993b), because the correlation coefficient was approximately 0.8. Furthermore, the time delay indicated that the oscillation of the separation point precedes the movement of the separation shock. Correlations between time histories of the separation and reattachment locations (defined by the locations of zero skin friction) show that the oscillations in the separation and reattachment points are correlated (peak coefficient of 0.3), and the reattachment motions precede those of the separation point. This latter observation is consistent with many previous compression ramp studies (e.g., Erengil & Dolling 1993b, Thomas et al. 1994). Wu & Martin's simulations also revealed the presence of upstream superstructures, which did affect the separation line, but their effect was restricted to inducing a smaller-scale spanwise wrinkling of the separation line as was observed by Wu & Miles (2001). The large-scale motion seemed to be driven by another mechanism.

These observations led Wu & Martin (2008) to suggest the following model of the unsteadiness. Upstream boundary layer structures cause smaller-scale unsteadiness, whereas large-scale motion is driven by pulsations of the separated flow. They argued that pulsations may be driven

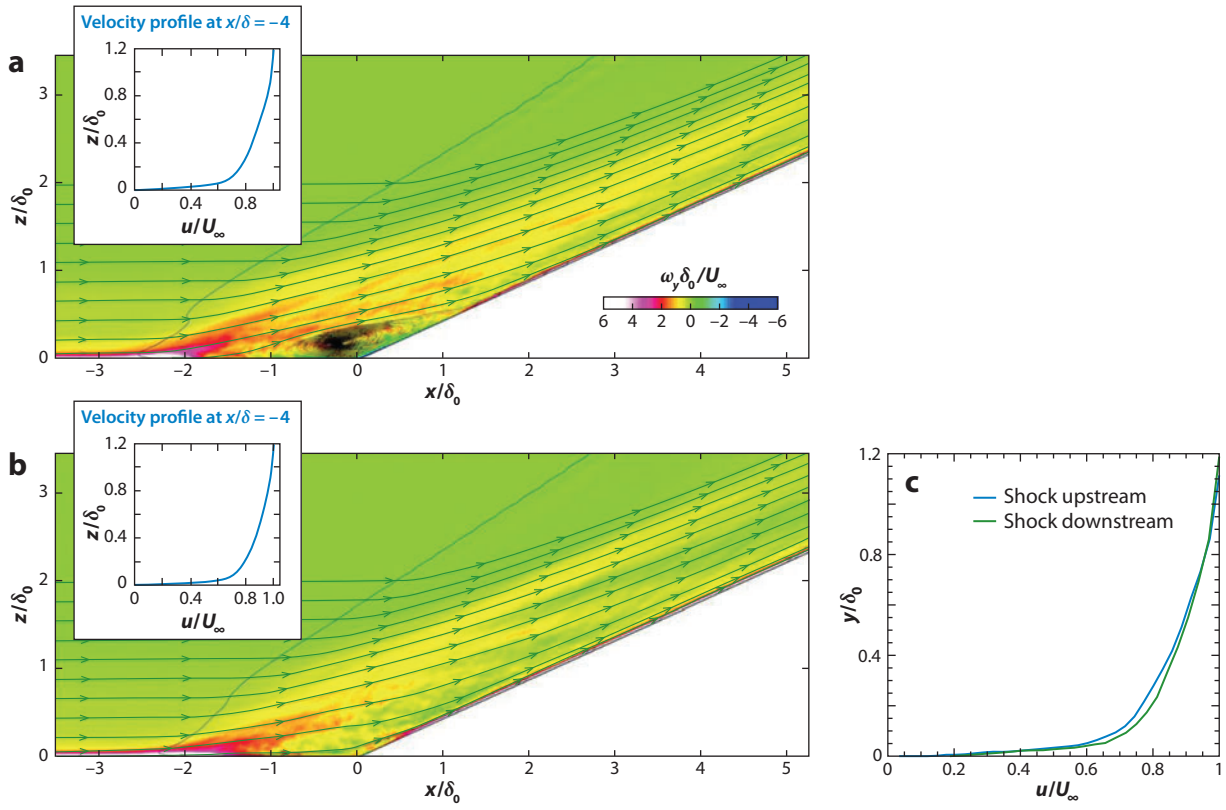

Figure 7

Direct numerical simulation results of a Mach 3 compression ramp interaction by Priebe & Martin (2012). The images represent streamwise-transverse planes of the spanwise vorticity, and several streamlines are shown. The separation shock is also shown in each image. The images have been spanwise averaged. (*a*,*b*) Two frames (frame 87 and 247, respectively) from a bubble-collapse event in Priebe & Martin (2012, supplementary movie 1). (*c*) Upstream boundary layer velocity profiles taken at a location of $x/\delta_0 = -4$ corresponding to both separation shock states in panels *a* and *b*. Panels *a* and *b* adapted with permission from Priebe & Martin (2012, supplementary movie 1). Copyright © 2012 Cambridge University Press.

by an instability that is similar to the wake flow instability that characterizes cavity flows. They argued that the shear layer may flap in response to an imbalance in (*a*) the entrainment rate of the shear layer and (*b*) the separation bubble recharge rate near reattachment. Wu & Martin's (2008) model is quite similar to the mechanism proposed by Piponniau et al. (2009) as it is based on an entrainment/recharge mechanism of the separated shear layer. The recent work of Priebe & Martin (2012) corroborated the findings of Wu & Martin (2008) and others on the dominant role of separation bubble pulsations on the separation shock motion by showing significant changes in the streamline organization, shear layer turbulence levels, and the size of the separation bubble, at different phases of SBLI unsteadiness. We note that the supplemental movies included in Priebe & Martin (2012) are very informative and are an excellent means to explore the interaction dynamics. For example, **Figure 7** shows two frames taken from Priebe & Martin (2012, supplementary movie 1), which represent approximately the start and end of an event where the separation bubble undergoes near complete collapse. **Figure 7*a*,*b*** shows vorticity fields that have been spanwise averaged to effectively filter out the effects of small-scale turbulent fluctuations on the dynamics.

In **Figure 7*a***, the bubble is large and the separation shock is located upstream, whereas in **Figure 7*b***, the bubble has collapsed and the separation shock moves approximately $0.5\delta_0$ downstream. The movie reveals interesting features during this event, such as the large-scale flapping of the shear layer and how the downstream sweep of the separation shock significantly lags behind the collapse of the bubble. Priebe & Martin (2012) also specifically discussed the changes in the turbulence activity in the shear layer at different phases of the oscillation cycle, which appear to support the shear layer entrainment model of Wu & Martin (2008) and Piponniau et al. (2009).

5. DISCUSSION

We see above that recent studies have greatly enhanced what is known about the driving mechanism of the low-frequency unsteadiness of shock-induced turbulent separated flows. Although there remain some outstanding questions, a consensus is being reached by groups whose views were quite divergent just a few years ago. This emerging consensus view is that strong interactions, which exhibit large separation bubbles, are primarily driven by a downstream instability, whereas weakly separated interactions can be strongly influenced by fluctuations in the upstream boundary layer. This concept was first addressed explicitly by Souverein et al. (2009) and Clemens & Narayanaswamy (2009) at the same American Institute for Aeronautics and Astronautics conference and was later published by Souverein et al. (2010).

Before continuing, it is helpful to point out that the understanding of this topic has been hindered by different uses of the term incipient separation in the literature. For example, Dussauge & Piponniau (2008), Piponniau et al. (2009), and Souverein et al. (2010) defined incipient separated flows as those that exhibit no mean reverse flow, irrespective of the relative size of the interaction length scale. In these studies, reverse flow was detected by using the PIV technique. We use the term incipient separation in the same context as Settles et al. (1979), who conducted one of the earliest comprehensive studies of the mean flow structure of different strength compression ramp interactions. Settles et al. (1979) showed that as the ramp angle was increased, the oblique shock would increasingly stand off from the ramp corner. The flow condition when the shock first began to stand off from the corner was termed "incipient" separation, and this condition had no discernible separation line in the surface streak line visualization (oil flow) and no reverse flow as inferred by the wall shear stress. Similarly, Simpson (1989) defined incipient separation as a flow that exhibits reverse flow less than 1% of the time. Settles et al. (1979) further showed that as the ramp angle was increased, the shock stand-off distance increased, the distance between the separation and reattachment lines in the surface flow visualization increased, and the region of negative skin friction increased. In Settles et al.'s (1979) definition of incipient separation, the incipient case indeed has no mean reverse flow, but it also has no separation shock (because the shock is attached to the corner), and the surface flow visualization indicates no separation and reattachment lines. If we now take the case of Hou et al. (2003), who used PIV to study the unsteadiness of a 24° compression ramp interaction in a Mach 2 flow, the separation shock was located $3\delta_0$ upstream of the corner, and a clear separation line in the surface flow visualization was located $2\delta_0$ upstream of the compression corner (see Hou 2003). According to Settles et al. (1979), an interaction of this strength is separated and exhibits mean reverse flow. Hou et al. (2003) attributed the lack of mean reverse flow to inadequate spatial resolution of the PIV technique. This is plausible as Settles et al. (1976) showed that reverse flow was restricted to a small region near the corner for elevations of approximately $0.1\delta_0$ from the wall, and this would have been too close to the wall for Hou et al. (2003) to resolve.

Although our use of the term incipient differs from the use by Dussauge & Piponniau (2008), Piponniau et al. (2009), and Souverein et al. (2010), there is really no disagreement on the broad

point that the strength or relative size of separation determines the degree to which an interaction exhibits sensitivity to upstream fluctuations. For example, Clemens & Narayanaswamy (2009) summarized studies that have looked at mechanisms of low-frequency unsteadiness. They observed the trend that studies exhibiting the highest influence of the upstream boundary layer tended to have separated flow length scales of $2\delta_0$ and below. Similarly, interactions that exhibited evidence for a predominantly downstream mechanism tended to have separated flow length scales of $4\delta_0$ and larger. Furthermore, the success of the model developed by Piponniau et al. (2009), which collapses unsteadiness frequencies over a wide range of Mach numbers, from subsonic to high supersonic, is strong evidence that the separated flow is driven by an instability associated with the entrainment of the separation bubble. The DNS results of Priebe & Martin (2012) also support this view as their low-pass filtered data quite clearly show a low-frequency flapping of the shear layer.

Here we argue that both upstream and downstream mechanisms are at work in all interactions, whether strongly separated or not, but the degree of influence of the upstream boundary layer fluctuations decreases with increasing separation scale. We take this view because in all studies that have looked for both an upstream and a downstream mechanism, both mechanisms have been seen to play a role, although with varying importance. For example, in the model of Piponniau et al. (2009), the scaling law collapses unsteadiness data for strong interactions but also for weak ones (e.g., Erengil & Dolling 1993b, Thomas et al. 1994), which the authors would consider incipient, so they should be dominated by the upstream boundary layer fluctuations. However, the success of the entrainment model indicates that the same entrainment instability is likely to be at work in these weaker interactions. The same argument can be made regarding the scaling analysis of Gonsalez & Dolling (1993), as they showed that a wide range of interactions (of varying strength) exhibits largely the same shock-foot Strouhal number (**Figure 3**). The success of these universal scaling laws implies a similarity of physics for weak and strong interactions.

Furthermore, in Wu & Martin (2008) and Priebe & Martin (2012), the separation length scales were $L_{sep}/\delta_0 = 4$ and 3, respectively, or strongly separated and moderately separated. As discussed previously, both groups of authors reported strong correlations between downstream fluctuations and separation shock motion. But it is important to point out that Wu & Martin (2008) showed a 30% correlation between mass flux fluctuations in the upstream boundary layer and separation shock motion. Although not as strong as other correlations that they measured, it is still substantial. Furthermore, Priebe & Martin (2012) investigated the coherence of different signals and concluded that the strongest coherence is between downstream quantities; however, it is quite interesting that the signature of the upstream influence is still present in their results. For example, the two frames shown in **Figure 7*a*,*b*** are taken from a single bubble-collapse event. If one carefully inspects the supplemental movies in Priebe & Martin (2012), it is quite clear that the velocity profile in the upstream boundary layer is correlated with the size of the separation bubble. For example, **Figure 7*c*** shows the boundary layer profiles corresponding to these two frames plotted together. The velocity profile in the lower part of the boundary layer is fuller by approximately 3% of U_∞ when the bubble has collapsed. A viewing of multiple events reveals a similar trend. It is interesting that the velocity difference is largest in the lower third of the boundary layer, which is similar to observations made by Beresh et al. (2002), who measured approximately a 2.5% U_∞ difference in velocity for downstream sweeps of the separation shock, and Hou (2003), who measured a 4% difference in the velocity for upstream and downstream shock-foot locations. Additionally, as discussed above, Souverein et al. (2010) measured similar magnitude differences for their weaker interaction and a 1–2% difference in a stronger interaction.

Now, just because the separated flow scale is correlated with changes in the upstream boundary layer does not imply it is a dominant mechanism. We can conduct a simple analysis to see if the

magnitude of fluctuations in the upstream boundary layer is large enough to cause a change in the downstream separated flow. In **Figure 7*a*,*b***, as the bubble collapses, the streamlines near the wall are forced to undergo a sharper turn that is more similar to the inviscid case, and this leads to an increase in pressure near the ramp corner. The wall-pressure time trace at a location of $x/\delta_0 = -1.5$ is provided by Priebe & Martin (2012), illustrating that the pressure increased by approximately $\Delta P_w = 0.3P_\infty$ during this event. Note that this bubble-collapse event occurs over a timescale of approximately $45\delta_0/U_\infty$. For the upstream boundary layer to be effective at causing the collapse of the separation bubble, the fluctuating momentum transfer rate must be large enough to overcome the pressure rise associated with the more compressed flow. We can do a simple analysis to investigate this possibility. In the upstream boundary layer to first order, the momentum transfer rate varies by $\dot{m}u'$. From **Figure 7*c***, we see that the region of velocity difference extends over approximately $0.4\delta_0$, which is approximately the same size as the separation bubble, which we will call area A. Therefore, we can write the fluctuation in the momentum transfer rate as

$$\dot{m}u' = \bar{\rho}\bar{u}Au'.$$

For simplicity, the mean density and velocity maintain their free-stream values, and we have

$$\dot{m}u' = \frac{P_\infty}{RT_\infty}u_\infty Au' = \gamma P_\infty M_\infty^2 A\frac{u'}{u_\infty}.$$

Now, for a pressure change of ΔP_w in the separation region, the force to be overcome as the shock moves downstream is $\Delta P_w A$. Taking the ratio of the momentum transfer rate fluctuation and the pressure force change, we obtain

$$\begin{aligned}\frac{\text{momentum transfer rate fluctuation}}{\text{change in pressure force}} &= \frac{\gamma P_\infty M_\infty^2 A\frac{u'}{u_\infty}}{\Delta P_w A} \\ &= \gamma M_\infty^2 \frac{1}{\Delta P_w/P_\infty}\frac{u'}{u_\infty}.\end{aligned} \quad (1)$$

Using Equation 1, $M_\infty = 2.9$, $\Delta P_w/P_\infty = 0.3$, and $u'/u_\infty = 0.03$, this ratio evaluates approximately to unity. This analysis shows that it is at least plausible that fluctuations of order 3% of the free-stream value could play a role in the separated flow dynamics, although the low coherence (approximately 0.25) between the mass flux fluctuations and the separation shock motion tells us that this is not a dominant mechanism (Priebe & Martin 2012). This analysis also suggests that upstream boundary layer fluctuations should be less effective at influencing stronger interactions because the upstream fluctuations should not change in magnitude, whereas the separated flow pressure changes will increase substantially. This analysis further implies that the momentum fluctuation must persist long enough to cause the required change, which is of order $45\delta_0/U_\infty$. It is important to emphasize that the velocity profiles in **Figure 7*c*** are spanwise averaged, so any superstructures would nominally be averaged out. Instead, the boundary layer must be undergoing low-frequency motions across the entire span.

The analysis above focuses on the mechanism of momentum fluctuations directly influencing the separated flow. However, there is a more indirect way that turbulent structures in the upstream boundary layer could play a role in the interaction dynamics. In particular, it is possible for turbulent fluctuations of the right frequency to force the global instability that drives the separated flow instability. In this way, relatively small upstream perturbations could seed an instability and thus amplify the fluctuations. Na & Moin (1998) discussed a similar mechanism in the DNS of a highly separated incompressible turbulent boundary layer. Their flow is massively separated as it is approximately 20 boundary layer thicknesses in extent. They showed that the instantaneous separation line strongly reflects variations in wall shear stress in the upstream boundary layer.

Furthermore, they observed large-scale, low-frequency unsteadiness related to large-scale turbulent structures in the separated shear layer that cause a flapping of the reattachment point. Interestingly, they observed that the shear layer structures originate in the upstream boundary layer but then grow in scale and in coherence as they propagate downstream toward the reattachment point. The separation and reattachment points were correlated, but the reattachment point fluctuations exhibited lower-frequency motions than the separation point.

This observation is quite interesting because it provides a means for the reattachment point to be influenced by the upstream flow, even though the separation line (or shock foot) is not influenced by the same fluctuations. Chong et al. (1998) also used DNS to study an incompressible separated flow and showed that the shear layer over the separation bubble is dominated by vorticity that originates in the lower one-tenth of the boundary layer. This observation can also be seen in the DNS of Priebe & Martin (2012) (see **Figure 7**), in which the high-vorticity region extending to approximately $0.1\delta_0$ from the wall is primarily responsible for the vorticity present in the separated shear layer. This observation is potentially important because we have also seen that the separated flow scale correlates with velocity fluctuations in the lower part of the upstream boundary layer (Beresh et al. 2002). Therefore, fluctuations near the wall may optimally seed the shear layer with structures that are most likely to lead to large-scale flapping.

An important question to consider is, what role do superstructures play in driving the separated flow unsteadiness of either weak or strong interactions? Although Ganapathisubramani et al. (2007, 2009) demonstrated a strong correlation between fluctuations induced by these structures and a separation line surrogate, it is also true that Touber & Sandham (2009) specifically suppressed the formation of such large-scale structures in their simulation but still obtained large-scale unsteadiness in agreement with previous experimental studies. If the upstream boundary layer fluctuations are indeed seeding the downstream instability, then it is only those fluctuations at the natural frequency of oscillation (St of approximately 0.03) that will be effective. Let us consider the case of a compression ramp with increasing angle: At small angles, the separation bubble will be small, so the frequency band to which it will be receptive will be relatively high; in contrast, as the bubble grows, the receptive frequency band will decrease. So it may be that the superstructures happen to be at the right frequency for the interaction studied by Ganapathisubramani et al. (2007, 2009), but those same structures may not be effective at driving much smaller or larger separated flows. This suggests that the presence of superstructures may represent a broader truth that low-frequency content in the upstream boundary layer is important, but perhaps the exact nature of these structures is not that critical. In other words, superstructures may be simply a manifestation of the low-frequency unsteadiness that is present at the wall of the upstream boundary layer.

We conclude this section with a discussion of a model proposed by Touber & Sandham (2011), which has a great deal of explanative power. Touber & Sandham (2011) started with the Reynolds-averaged Navier-Stokes equations and showed that a reduced-order model of the separated flow system dynamics could be obtained. They demonstrated that the separation shock responded to disturbances as a first-order system, similar to Plotkin (1975). They first sought to understand the necessity of organized motions in the incoming boundary layer in driving the interaction and demonstrated that it exhibited low-frequency pulsations very similar to a canonical SBLI, even when the fluctuations in the incoming boundary layer were represented by a white-noise spectrum. Interestingly, they found that removing the low-frequency fluctuations in the incoming boundary layer by high-pass filtering the input fluctuations resulted in the SBLI losing its low-frequency pulsations, hence showing the need for low-frequency fluctuations to drive the separation bubble pulsations. In other words, the instability of the system (the global instability) is not self-sustaining and needs an external driving source. The authors emphasized that the origin of the forcing needs to be at the natural frequency of the system, and this could be in the form of coherent or incoherent

motions in the upstream boundary layer, fluctuations in the downstream separated flow, or simply broadband noise in the background.

This view of the shock-induced separated flow as a forced dynamical system is particularly appealing because it seems to explain or incorporate many observations that have been made of SBLI dynamics in the literature. For example, in this view the separation bubble has a preferred oscillation frequency that is driven by external disturbances, including those in the upstream boundary layer. Therefore, it would be expected that correlations among either upstream or downstream fluctuations and the separation bubble pulsations could be found. Furthermore, it would be expected that the turbulent boundary layer would become a weaker forcing function with increasing separation bubble size because of the momentum considerations discussed earlier in this section.

6. FUTURE WORK

Although much has been learned about the dynamics of SBLIs over the past 20 years, there remains a rich set of issues for future researchers to address. Future work can be directed at refining and improving our knowledge of separated flow dynamics in canonical interactions, and improving our knowledge of the unsteadiness of more complex flows relevant to practical applications. Below we briefly mention some topics for which further research is particularly warranted.

6.1. Three-Dimensional Effects

Strong interactions, with large separated flow length scales, are problematic for experimental testing owing to the finite width of wind tunnels. For example, Dupont et al. (2005) showed that their strong reflected shock interactions were influenced by the tornado vortices induced by the incident shock interacting with the tunnel side walls and corner flows. Bruce et al. (2011) studied the effect of the corner flows on reflected normal shock interactions and showed that the mean structure of the interactions is greatly influenced by the state of the corner boundary layers. The extent to which 3D effects may influence separated flow unsteadiness is not yet well understood but is critically important for practical geometries. Furthermore, the class of inherently 3D open separated flows, such as those generated by swept interactions, needs to be studied as deeply as 2D interactions have been. Understanding how the vortical separated flow affects the large-scale unsteadiness would be particularly illuminating.

6.2. System Dynamics

If external disturbances do indeed serve as a forcing function for the low-frequency dynamics, then it would be beneficial to understand better how such disturbances affect the flow. For example, it may be beneficial to add different types of pulsed disturbances to the upstream boundary layer or in the downstream separated flow to determine how the interaction responds. Such an approach was taken by Narayanaswamy et al. (2012), who forced a compression ramp interaction with upstream high-frequency pulsed-plasma jet actuators and showed a strong influence on the separation shock unsteadiness.

6.3. Separated Flow Dynamics Scaling

Although recent work has led to plausible models of large-scale unsteadiness, a more detailed understanding of the physics is still required. It would be beneficial to study a wider range of canonical

separated interactive flows to test the generality of proposed mechanisms or to reveal new, as yet undiscovered mechanisms. For example, most experiments have been conducted in similarly sized wind tunnels, but it would be useful to see if previously determined scaling relationships hold for much larger-scale flows or at significantly higher Reynolds numbers.

6.4. Interactions in Internal Flows

Although a great deal of information is known about canonical interactions in external flows, the same level of knowledge has not been developed for internal flows, such as in supersonic inlets and isolators. In these internal flows, multiple reflected shocks are typically present that can cause boundary layer separation to occur at multiple locations on the floor/ceiling and channel side walls. These multiple regions of separation have the potential to interact in complex ways. Furthermore, in some cases, there is a subsonic downstream boundary condition, and thus the flow unsteadiness can be coupled to fluctuations at the channel exit.

7. CONCLUSION

Above we survey some recent studies that have specifically addressed the question of what drives the low-frequency unsteadiness of simple-geometry separated shock wave/boundary layer interactions. A wealth of past and recent results suggests that the unsteadiness is driven either by fluctuations in the upstream boundary layer or by some large-scale instability intrinsic to the separated flow. Based on this review, we conclude that both mechanisms are always present in all shock-induced turbulent separated flows but that the downstream mechanism dominates for strongly separated flows, and a combined mechanism dominates for weakly separated flows. Strong separation is expected for high inviscid shock strength and low Reynolds numbers of the undisturbed boundary layer. High–Reynolds number boundary layers will tend to be more resistant to separation and so tend to exhibit smaller separated flows. As proposed by several groups, it appears that for strong separation, the bubble pulsates in response to a global instability that leads to flapping of the reattachment point. The reattachment point fluctuations cause expansion/contraction of the bubble and a synchronous movement of the separation line, separation shock (outside the boundary layer), and separation shock foot. For weaker separation, turbulent fluctuations are correlated with separation bubble dynamics, but the exact role they play is not well understood. The upstream fluctuations in momentum either could directly lead to expansion/reduction in the separation bubble or may simply seed the shear layer with disturbances that grow and lead to large-scale flapping. Regardless, a scaling analysis suggests that the upstream momentum fluctuations are large enough to directly collapse the separation bubble in weakly separated flows but not in strongly separated ones. The role of coherent structures in the upstream boundary layer is not clear, but the evidence suggests that the exact nature of the upstream fluctuations is not as important as their frequency and magnitude. We find the model proposed by others that the separated flow acts as a low-order dynamical system that is forced by the upstream boundary layer (and downstream fluctuations as well) to be particularly appealing because it is in general agreement with the observations and mechanisms described above.

DISCLOSURE STATEMENT

The authors are not aware of any biases that might be perceived as affecting the objectivity of this review.

ACKNOWLEDGMENTS

N. Clemens would like to thank his former colleague David Dolling for many years of productive collaboration on the physics of shock-induced turbulent separation. N. Clemens would also like to thank former students and postdocs who worked on this topic, including Steve Beresh, Yongxi Hou, Haldun Ünalmis, Pablo Bueno, Justin Wagner, and Bharath Ganapathisubramani. Our past work on this topic has been supported by grants from ARO and AFOSR. These sources of support are gratefully acknowledged.

LITERATURE CITED

Adrian RJ, Meinhart CDS, Tomkins CD. 2000. Vortex organization in the outer region of the turbulent boundary layer. *J. Fluid Mech.* 422:1–54

Andreopoulos Y, Agui JH, Briassulis G. 2000. Shock wave-turbulence interactions. *Annu. Rev. Fluid Mech.* 32:309–45

Andreopoulos J, Muck KC. 1987. Some new aspects of the shock-wave boundary layer interaction. *J. Fluid Mech.* 32:309–45

Babinsky H, Harvey JK, eds. 2011. *Shock Wave–Boundary-Layer Interactions*. Cambridge, UK: Cambridge Univ. Press

Beresh SJ, Clemens NT, Dolling DS. 2002. Relationship between upstream boundary layer velocity fluctuations and separation shock unsteadiness. *AIAA J.* 40:2412–22

Bruce PJK, Burton DMF, Titchener NA, Babinsky H. 2011. Corner effect and separation in transonic channel flows. *J. Fluid Mech.* 679:247–62

Brusniak L, Dolling DS. 1994. Physics of unsteady blunt-fin-induced shock wave/turbulent boundary layer interactions. *J. Fluid Mech.* 273:375–409

Chong MS, Soria J, Perry AE, Chacin J, Cantwell BJ, Na Y. 1998. Turbulence structures of wall-bounded shear flows found using DNS data. *J. Fluid Mech.* 357:225–47

Clemens NT, Narayanaswamy V. 2009. *Shock/turbulent boundary layer interactions: review of recent work on sources of unsteadiness*. Presented at AIAA Fluid Dyn. Meet., 39th, San Antonio, AIAA Pap. 2009-3710

Delery J, Marvin J. 1986. *Shock-Wave Boundary Layer Interactions*. AGARDograph 280. Brussels: NATO

Doerffer P, Hirsch C, Dussauge JP, Babinsky H, Barakos GN, eds. 2010. *Unsteady Effects of Shock Wave Induced Separation*. New York: Springer

Dolling DS. 1993. *Fluctuating loads in shock-wave/boundary layer interaction: tutorial and update*. Presented at AIAA Aerosp. Sci. Meet. Exhib., 31st, Reno, NV, AIAA Pap. 1993-0284

Dolling DS. 1998. High-speed turbulent separated flows: consistency of mathematical models and flow physics. *AIAA J.* 36:725–32

Dolling DS. 2001. Fifty years of shock wave/boundary layer interaction: what next? *AIAA J.* 39:1517–31

Dolling DS, Brusniak L. 1989. Separation shock motion in fin, cylinder, and compression ramp-induced turbulent interactions. *AIAA J.* 27:734–42

Dolling DS, Murphy MT. 1983. Unsteadiness of the separation shock wave structure in a supersonic compression ramp flowfield. *AIAA J.* 21:1628–34

Dupont P, Haddad C, Ardissone JP, Debiève JF. 2005. Space and time organization of a shock wave/turbulent boundary layer interaction. *Aerosp. Sci. Technol.* 9:561–72

Dupont P, Haddad C, Debiève JF. 2006. Space and time organization in a shock-induced separated boundary layer. *J. Fluid Mech.* 559:255–77

Dussauge JP, Piponniau S. 2008. Shock/boundary-layer interactions: possible sources of unsteadiness. *J. Fluids Struct.* 24:1166–75

Edwards JR. 2008. *Numerical simulations of shock/boundary layer interactions using time-dependent modeling techniques: a survey of recent results*. Presented at AIAA Aerosp. Sci. Meet. Exhib., 46th, Reno, NV, AIAA Pap. 2008-525

Erengil ME, Dolling DS. 1991a. Correlation of separation shock motion with pressure fluctuations in the incoming boundary layer. *AIAA J.* 29:1868–77

Erengil ME, Dolling DS. 1991b. Unsteady wave structure near separation in a Mach 5 compression ramp interaction. *AIAA J.* 29:728–35

Erengil ME, Dolling DS. 1993a. Effects of sweepback on unsteady separation in Mach 5 compression ramp interactions. *AIAA J.* 31:302–11

Erengil ME, Dolling DS. 1993b. *Physical causes of separation shock unsteadiness in shock wave turbulent boundary layer interactions.* Presented at AIAA Fluid Dyn. Conf., 24th, Orlando, FL, AIAA Pap. 1993-3134

Ganapathisubramani B, Clemens N, Dolling D. 2007. Effects of upstream boundary layer on the unsteadiness of shock-induced separation. *J. Fluid Mech.* 585:369–94

Ganapathisubramani B, Clemens NT, Dolling D. 2009. Low-frequency dynamics of shock-induced separation in a compression ramp interaction *J. Fluid Mech.* 636:397–436

Gonsalez JC, Dolling DS. 1993. *Correlation of interaction sweepback effects on the dynamics of shock-induced turbulent separation*. Presented at AIAA Aerosp. Sci. Meet. Exhib., 31st, Reno, NV, AIAA Pap. 1993-0776

Gramman RA, Dolling DS. 1990. Detection of turbulent boundary-layer separation using fluctuating wall pressure signals. *AIAA J.* 28:1052–56

Gramman RA, Dolling DS. 1992. *A preliminary study of the turbulent structures associated with unsteady separation shock motion in a Mach 5 compression ramp interaction.* Presented at Aerosp. Sci. Meet. Exhib., 30th, Reno, NV, AIAA Pap. 1992-0744

Hou YX. 2003. *Particle image velocimetry study of shock induced turbulent boundary layer separation*. PhD diss. Univ. Texas, Austin

Hou YX, Clemens NT, Dolling DS. 2003. *Wide-field PIV study of shock induced turbulent boundary layer separation*. Presented at AIAA Aerosp. Sci. Meet. Exhib., 41st, Reno, NV, AIAA Pap. 2003-0441

Humble RA, Elsinga GE, Scarano F, van Oudheusden BW. 2007a. Experimental investigation of the three-dimensional structure of a shock wave/turbulent boundary layer interaction. *Proc. 16th Aust. Fluid Mech. Conf.*, ed. P Jacobs, T McIntyre, M Cleary, D Buttsworth, D Mee, et al., pp. 729–36. Melbourne: Aust. Fluid Mech. Soc.

Humble RA, Elsinga GE, Scarano F, van Oudheusden BW. 2007b. *Investigation of the instantaneous 3D flow organization of a shock wave/turbulent boundary layer interaction using tomographic PIV*. Presented at AIAA Fluid Dyn. Conf. Exhib., 37th, Miami, AIAA Pap. 2007-4112

Humble RA, Elsinga GE, Scarano F, van Oudheusden BW. 2009. Three-dimensional instantaneous structure of a shock wave/turbulent boundary layer interaction. *J. Fluid Mech.* 622:33–62

Humble RA, Scarano F, van Oudheusden. 2007c. Particle image velocimetry measurements of a shock wave/turbulent boundary layer interaction. *Exp. Fluids* 43:173–83

Hutchins N, Marusic I. 2007. Evidence of very long meandering structures in the logarithmic region of turbulent boundary layers. *J. Fluid Mech.* 579:1–28

Kim KC, Adrian RJ. 1999. Very large-scale motion in the outer layer. *Phys. Fluids* 11:417–22

Knight DD, Degrez G. 1998. *Shock wave boundary layer interactions in high Mach number flows, a critical survey of current numerical prediction capabilities*. Advis. Rep. 319, AGARD, Neuilly sur Seine

Knight DD, Horstman CC, Shapey B, Bogdonoff S. 1987. Structure of supersonic turbulent flow past a sharp fin. *AIAA J.* 25:1331–37

Knight DD, Yan H, Panaras AG, Zheltovodov A. 2003. Advances in CFD prediction of shockwave turbulent boundary layer interactions. *Prog. Aerosp. Sci.* 39:121–84

Lee BHK. 2001. Self-sustained oscillations on airfoils at transonic speeds. *Prog. Aerosp. Sci.* 37:147–96

McClure WB. 1992. *An experimental study of the driving mechanism and control of the unsteady shock induced turbulent separation in a Mach 5 compression corner flow*. PhD thesis. Univ. Texas, Austin

Morgan B, Kawai S, Lele SK. 2010. *Large-eddy simulation of an oblique shock impinging on a turbulent boundary layer*. Presented at AIAA Fluid Dyn. Conf., 40th, Chicago, AIAA Pap. 2010-4467

Na Y, Moin P. 1998. Direct numerical simulation of a separated turbulent boundary layer. *J. Fluid Mech.* 374:379–405

Narayanaswamy V, Raja LL, Clemens NT. 2012. Control of unsteadiness of a shock wave/turbulent boundary layer interaction by using a pulsed-plasma jet actuator. *Phys. Fluids* 24:076101

Piponniau S, Dussauge JP, Debiève JF, Dupont P. 2009. A simple model for low-frequency unsteadiness in shock-induced separation. *J. Fluid Mech.* 629:87–108

Pirozzoli S, Grasso F. 2006. Direct numerical simulation of impinging shock wave/turbulent boundary layer interaction at $M = 2.25$. *Phys. Fluids* 18:065113
Plotkin KJ. 1975. Shock wave oscillation driven by turbulent boundary layer fluctuations. *AIAA J.* 13:1036–40
Poggie J, Smits AJ. 2001. Shock unsteadiness in a reattaching shear layer. *J. Fluid Mech.* 429:155–85
Priebe S, Martin MP. 2012. Low-frequency unsteadiness in shock wave–turbulent boundary layer interaction. *J. Fluid Mech.* 699:1–49
Ringuette MJ, Bookey P, Wyckham C, Smits AJ. 2009. Experimental study of a Mach 3 compression ramp interaction at $Re_\theta = 2400$. *AIAA J.* 47:373–85
Schmisseur JD, Dolling DS. 1994. Fluctuating wall pressures near separation in highly swept turbulent interactions. *AIAA J.* 32:1151–57
Settles GS, Fitzpatrick TJ, Bogdonoff SM. 1979. Detailed study of attached and separated compression corner flowfields in high Reynolds number supersonic flow. *AIAA J.* 17:579–85
Settles GS, Vas IE, Bogdonoff SM. 1976. Details of a shock-separated turbulent boundary layer at a compression corner. *AIAA J.* 14:1709–15
Simpson RL. 1989. Turbulent boundary layer separation. *Annu. Rev. Fluid Mech.* 21:205–34
Smits AJ, Dussauge JP. 1996. *Turbulent Shear Layers in Supersonic Flow*. Woodbury, NY: AIP
Souverein LJ, Dupont P, Debiève JF, Dussauge JP, van Oudheusden BW, Scarano F. 2009. Effect of interaction strength on the unsteady behavior of shock wave boundary layer interactions. Presented at AIAA Fluid Dyn. Conf., 29th, San Antonio, TX, AIAA Pap. 2009-3715
Souverein LJ, Dupont P, Debiève JF, Dussauge JP, van Oudheusden BW, Scarano F. 2010. Effect of interaction strength on unsteadiness in turbulent shock-wave induced separations. *AIAA J.* 48:1480–93
Thomas FO, Putnam CM, Chu HC. 1994. On the mechanism of unsteady shock oscillation in shock wave/turbulent boundary layer interactions. *Exp. Fluids* 18:69–81
Tomkins CD, Adrian RJ. 2003. Spanwise structure and scale growth in turbulent boundary layers. *J. Fluid Mech.* 490:37–74
Touber E, Sandham ND. 2009. Large-eddy simulation of low-frequency unsteadiness in a turbulent shock-induced separation bubble. *Theor. Comput. Fluid Dyn.* 23:79–107
Touber E, Sandham ND. 2011. Low-order stochastic modelling of low-frequency motions in reflected shock-wave/boundary-layer interactions. *J. Fluid Mech.* 671:417–65
Ünalmis OH, Dolling DS. 1994. *Decay of wall pressure field structure of a Mach 5 adiabatic turbulent boundary layer*. Presented at AIAA Fluid Dyn. Conf., 25th, Colorado Springs, AIAA Pap. 1994-2363
Wu M, Martin MP. 2008. Analysis of shock motion in shockwave and turbulent boundary layer interaction using direct numerical simulation data. *J. Fluid Mech.* 594:71–83
Wu P, Miles RB. 2001. Megahertz visualization of compression-corner shock structures. *AIAA J.* 39:1542–46
Zheltovodov A. 1996. *Shock wave/turbulent boundary layer interactions: fundamental studies and applications*. Presented at AIAA Fluid Dyn. Conf., 27th, New Orleans, AIAA Pap. 1996-1977

Annual Review of
Fluid Mechanics

Volume 46, 2014

Contents

Indexes

Errata

An online log of corrections to *Annual Review of Fluid Mechanics* articles may be found at http://fluid.annualreviews.org/errata.shtml